A method to relate initial elastic stress to fault population strains

Richard A. Schultz

Geomechanics-Rock Fracture Group, Department of Geological Sciences, Mackay School of Mines, University of Nevada, Reno, Nevada, USA

Received 27 November 2002; revised 21 February 2003; accepted 5 March 2003; published 13 June 2003.

[1] A relationship between the cumulative elastic driving stress (or far-field elastic differential stress) and the inelastic strain of a fault population can be defined from the displacement-length scaling relations of the population. Two solutions are presented: one in which the elastic parameters remain constant, and the other that assumes a progressive reduction in modulus with increasing fracture spatial density. The method is illustrated by using fault populations from Mars. Cumulative differential stresses of 37 MPa and 87 MPa (computed here for 1 km depth) are implied to have produced the strains observed at Amenthes Rupes (widely spaced thrust faults) and Tempe Terra (closely spaced normal faults), respectively. *INDEX TERMS:* 5475 Planetology: Solid Surface Planets: Tectonics (8149); 6225 Planetology: Solar System Objects: Mars; 8020 Structural Geology: Mechanics; 8010 Structural Geology: Fractures and faults; 8149 Tectonophysics: Planetary tectonics (5475). **Citation:** Schultz, R. A., A method to relate initial elastic stress to fault population strains, *Geophys. Res. Lett.*, *30*(11), 1593, doi:10.1029/2002GL016681, 2003.

1. Introduction

[2] Geodynamic models of brittle crustal deformation require a comparison between predicted magnitudes of stress and independent observations, typically measured strains, in order to assess their applicability to particular tectonic regimes. For example, plate bending models (e.g., for subduction zones or volcano loads) typically predict elastic stresses in the upper plate that exceed plausible values of rock strength, implying that fault and joint populations (i.e., inelastic brittle strain) will develop progressively as bending proceeds, making explicit comparisons of predicted stress and observed strain difficult. Similarly, the development of geodynamic models for the Tharsis region of Mars [e.g., *Banerdt et al.*, 1992; *Johnson and Phillips*, 2003] has been hindered by the absence of a rigorous correspondence between model predictions and the observed structures. In this case, predicted elastic stresses are loosely compared to inelastic fault population strains, resulting only in a qualitative assessment of the models. As a result, progress in planetary geodynamics has been fettered by the difficulty in relating elastic stress to brittle (inelastic) strain.

[3] In this paper I present a method that permits the large inelastic strains measured from typical fault populations to be compared quantitatively to values of elastic stress predicted by simple geodynamic models. Two cases are developed: one in which the elastic properties of a model (i.e., for the crust or lithosphere) are held constant during the deformation [e.g., *Banerdt et al.*, 1992; *Phillips et al.*, 2001] (see *Mège and Masson* [1996]), and the other, in which the elastic properties evolve with increasing brittle strain.

2. Fault Population Strain

[4] Calculation of brittle strain from fault populations is straightforward. Lengths L, down-dip heights H, and average (geologic) displacements D_{avg} are obtained for each (ith) fault in the population, with the summed product of these being the total geometric moment of the population, M_g. The scalar geologic (or seismic) moment [e.g., *Pollard and Segall*, 1987, p. 302] is $M_0 = M_g G$, where G is the average crustal shear modulus.

[5] The brittle strain ε is M_g normalized by the appropriate dimension of the faulted region having thickness T, area A, and volume $V = TA$. For "small" faults (having lengths L smaller than their downdip heights H) [e.g., *Scholz*, 1997], $H_i < T/\sin\delta_i$; for "large" faults (having $L > H$), $H_i = T/\sin\delta_i$, so the strain is obtained from Kostrov's formula (assuming constant fault dips) as

$$\varepsilon_n = \frac{2\sin 2\delta}{2\,AT}\sum_{i=1}^{N}\left[D_i L_i H_i\right] \quad \text{or} \quad \varepsilon_n = \frac{2\sin 2\delta}{2\,AT}\sum_{i=1}^{N}\left[D_i L_i \frac{T}{\sin\delta}\right] \quad (1)$$

In (1–4) the first expression is for small faults, the second for large faults. Using the trigonometric substitution $\sin 2\delta = (\cos\delta \sin\delta)$, the normal strain is [e.g., *Scholz*, 1997]

$$\varepsilon = \frac{\sin\delta\cos\delta}{V}\sum_{i=1}^{N}\left[D_{avg_i} L_i H_i\right] \text{ or } \varepsilon = \frac{\cos\delta}{A}\sum_{i=1}^{N}\left[D_{avg_i} L_i\right] \quad (2)$$

in which δ is fault dip angle. Here, M_g is calculated for the component of the complete moment tensor for the population in the horizontal plane and normal to fault strike [e.g., *Aki and Richards*, 1980, pp. 117–118; *Scholz*, 1997].

[6] Faults within a population are now understood to characteristically define $D_{max}/L = \gamma$ = constant [e.g., *Clark and Cox*, 1996; *Scholz*, 1997], including data sets from Earth [e.g., *Cowie et al.*, 1993], Mars [*Schultz*, 1999; *Wilkins et al.*, 2002], and Mercury [*Watters et al.*, 2000]. Particular values of γ depend on several variables including rock properties, driving stress, and geometric details of the fault population [e.g., *Cowie and Scholz*, 1992; *Schultz*, 1999]. By noting that the average displacement $D = \kappa D_{max}$, where $\kappa \sim 0.6$–0.7 [*Dawers et al.*, 1993; *Moore and Schultz*, 1999] the strain equations can be written as

$$\varepsilon = \frac{\kappa\gamma\sin\delta\cos\delta}{V}\sum_{i=1}^{N}\left[L_i^2 H_i\right] \text{ or } \varepsilon = \frac{\kappa\gamma\cos\delta}{A}\sum_{i=1}^{N}\left[L_i^2\right] \quad (3)$$

[see also *Wilkins et al.*, 2002].

Copyright 2003 by the American Geophysical Union.
0094-8276/03/2002GL016681$05.00

[7] The "spatial density" ρ_{fp} of a fracture population, defined from strain energy considerations, has been used in studies of crack strains [*Segall and Pollard*, 1983; *Segall*, 1984], joint set growth [*Olson*, 1993], compressive rock strength [*Kemeny and Cook*, 1986], fracture hydrology [*Renshaw*, 1997], and rock deformability [*Walsh*, 1965; *Kachanov*, 1992]. Noting that the dimensionless fracture density is given (following *Segall and Pollard* [1983] and *Kachanov* [1992]) by

$$\rho_{fp} \equiv \sum_{i=1}^{N} \left[\frac{L_i^2 H_i}{V}\right] \text{ or } \rho_{fp} \equiv \sum_{i=1}^{N} \left[\frac{L_i^2}{A}\right] \tag{4}$$

the strains are given compactly by

$$\varepsilon = \kappa\gamma f(\delta)\rho_{fp} \tag{5}$$

with $f(\delta)$ as in (2) or (3) for small or large faults, respectively. Equation (5) illustrates how brittle strain can increase as the fault population grows in size (e.g., aggregate length) at constant $D_{\max}/L$ [e.g., *Gupta and Scholz*, 2000a].

3. Fault Driving Stress: Incremental and Cumulative

[8] The driving stresses for a fault population to achieve strains given by (5) are estimated by using the relations for fracture displacements [e.g., *Pollard and Segall*, 1987]. For an individual fault within a population, having a central well-slipped portion bounded by frictionally stronger end zones (a "Dugdale-Barenblatt" model) [e.g., *Cowie and Scholz*, 1992],

$$D_{\max} = \frac{4(1-\nu^2)}{E}\sigma_d^* a \tag{6}$$

in which ν is Poisson's ratio, E is Young's modulus (both of the surrounding rock), a is fault half-length, and σ_d^* is the effective driving stress on the fault, including its yielded end zones, which is given by [*Schultz and Fossen*, 2002]

$$\sigma_d^* = \sigma_d - \sigma_y\left[1 - \cos\left(\frac{\pi}{2}\frac{\sigma_d}{\sigma_y}\right)\right] \tag{7}$$

in which σ_y is the yield strength of rock bounding the fault [e.g., *Cowie and Scholz*, 1992]. Letting $B = \sigma_y/\sigma_d$, (7) becomes

$$\sigma_d^* = \sigma_d\left\{1 - B\left[1 - \cos\left(\frac{\pi}{2}\frac{1}{B}\right)\right]\right\} = C\sigma_d \tag{8}$$

Here, σ_d is the driving stress on the yielded part of the fault (minus its end zones) [e.g., *Chell*, 1977]. With $L = 2a$, (6) becomes

$$\frac{D_{\max}}{L} = \gamma = \frac{2(1-\nu^2)}{E}C\sigma_d \tag{9}$$

and

$$\sigma_d = \frac{\gamma E}{2C(1-\nu^2)} \tag{10}$$

Plausible values of σ_y/σ_d are $B = 2-3$ [see *Cowie and Scholz*, 1992; *Schultz and Fossen*, 2002]. For $B = 2$, cos ($\pi/4$) in equation (8) = cos 45° and $\sigma_d^* = 0.4142\sigma_d$; for $B = 3$, $\sigma_d^* = 0.6\sigma_d$, so that $C = 0.4-0.6$. For faults in perfectly elastic rock ($\sigma_y \rightarrow \infty$), cos 0°, $\sigma_d^* = \sigma_d$, $C = 1.0$, and, with $L = 2a$, (9) reduces to the well-known case from Linear Elastic Fracture Mechanics [e.g., *Pollard and Segall*, 1987].

[9] The incremental driving stress ("stress drop") for one episode of fault slip (e.g., seismic) is $\sigma_d = \sigma_n(\mu_s - \mu_d)$, in which σ_n is the normal stress resolved onto the fault, μ_s is the maximum (or "static"), pre-slip friction coefficient, and μ_d is the post-slip ("dynamic") friction coefficient on the fault. Typical values of $\Delta\mu = (\mu_s - \mu_d)$, which corresponds to $-(a-b)$ for seismic events [*Scholz*, 1998], range between 10^{-2} and 10^{-3}. For values of $\mu_s = 0.6$ and $\mu_d = 0.59$ or 0.599 [e.g., *Marone*, 1998; *Scholz*, 1998], the incremental σ_d is perhaps 0.1–1% of σ_n on the fault. For example, an individual fault with $\sigma_n = 10$ MPa and $\Delta\mu = 0.01$ (a large stress drop) yields an incremental driving stress σ_d of 0.1 MPa; using $E = 50$ GPa, $\nu = 0.25$, and $C = 0.67$ in (9), $D_{\max}/L = \gamma = 1 \times 10^{-6}$, which is in the range of seismic events [*Scholz*, 1997].

[10] Cumulative driving stress represents the sum of the incremental driving stresses that collectively lead to the cumulative geologic offset measured on a fault. This quantity is defined as the ratio of γ for faults (e.g., 10^{-2}) to γ for earthquakes (e.g., 10^{-5}) times the incremental driving stress σ_d (for the earthquake). The cumulative driving stress for faults is, using these values, of order $(10^{-2}/10^{-5})$ (0.1 MPa) = 100 MPa [e.g., *Cowie and Scholz*, 1992; *Gupta and Scholz*, 2000b]. For example, using $E = 50$ GPa, $\nu = 0.25$, $C = 0.67$, $\delta = 30°$, and $f(\delta) = \cos\delta$ ("large" faults), in (10), $\sigma_d = 53.3$ MPa for $\gamma = 10^{-3}$, and 533 MPa for $\gamma = 10^{-2}$.

[11] As an illustration of cumulative driving stress, the number of slip events on a fault is given by

$$N = \frac{\sigma_d}{\sigma_n \Delta\mu} \tag{11}$$

For example, an individual fault with a cumulative driving stress σ_d of 53.3 MPa, σ_n of 10 MPa (averaged over the fault), and $\Delta\mu$ of 0.01 (a large stress drop) would require ~533 slip events to accumulate displacements of $D_{\max}/L = \gamma = 10^{-3}$. Although the size of an individual slip event would scale with the fault length L, the number of events is independent of L. The total number of slip events for all faults in the population would be equation (11) times the number of faults.

[12] To relate cumulative driving stress more fully to fault-population strain, the Young's modulus should reflect softening of the faulted rock mass over the deformed volume (for "small" faults) or area (for "large" faults). Reduction of modulus E with increasing crack density is well known [e.g., *Bieniawski*, 1993]. For example, E is reduced in the direction normal to an array of cracks or faults, whereas ν is relatively unaffected [e.g., *Jaeger and Cook*, 1979, pp. 329–337]. For a population of faults normal to their strike, E varies inversely with their spatial density, so that

$$E'_{pop} \approx E\exp\left(-\frac{\pi}{2}\rho_{fp}\right) \tag{12}$$

after *Kachanov* [1992]. This expression, along with others that differ somewhat in detail [*Kachanov*, 1992], suggests how the modulus of faulted rock (taken here as analogous to cracked rock) decreases with increasing values of spatial density. For $\rho_{fp} = 1.0$, the reduction in E for faulted rock is smaller by a factor of ~2 relative to cracked rock for the same fracture parameters [*Jaeger and Cook*, 1979, p. 332, 334].

4. Results

[13] We combine the expressions for brittle strain (5), cumulative fault driving stress (10), and reduced Young's modulus (12) through γ for the population, giving

$$\sigma_d = \left[\frac{E'_{pop}}{(1-\nu^2)}\right]\left[\frac{1}{2\kappa C f(\delta)\rho_{fp}}\right]\varepsilon \qquad (13)$$

Equation (13) estimates the cumulative driving stress required for the accumulation of displacements on faults within a population to brittle strains given by (5) using (5), (13) reduces to (10) for constant E.

[14] As more faults grow, ρ_{fp} increases and E'_{pop} decreases, modulating and reducing the cumulative driving stress required to increase brittle strain. This relationship, analogous to the post-peak region of laboratory compression tests on rock, is shown in Figure 1 for growth of a non-interacting (i.e., widely spaced) population of faults. "Large" spatial densities in engineering [e.g., *Kachanov*, 1992] are those exceeding $\rho_{fp} \sim 0.5$ (corresponding for $\gamma = 10^{-3}$ to strain of 0.03%); clearly, significantly greater values of ρ_{fp} are needed for geologic strains in the 1–10% range, as observed in extensional regions [e.g., *Gupta and Scholz*, 2000b] (note that *Renshaw* [1997] shows ρ_{fp} for hydrofractures that exceed 1.5–2; interacting but unlinked tectonic joints in the Sierra Nevada have $\rho_{fp} \sim 2.4$ [e.g., *Segall*, 1984]). The driving stress magnitude may stabilize (i.e., not decrease so markedly) with increasing strain for large values of ρ_{fp} due to fault interaction, linkage, and localization of strain onto particular faults; quantification of these effects is beyond the scope of this analysis (see *Borgos et al.* [2000] for discussion of these processes on the fault population statistics). Equation (13) is probably most useful for $\rho_{fp} < 0.5$.

[15] Using the relations for Coulomb frictional sliding ($|\tau| = \sigma_n \Delta\mu$) [e.g., *Jaeger and Cook*, 1979, pp. 95–96], the cumulative driving stress (10) can be recast into cumulative elastic differential stress. Using the principal stresses and substituting $[(\sigma_1 - \sigma_2)/2]\sin 2\phi$ (in which ϕ is either the fault dip δ (for thrust faults), or $(90° - \delta)$ (for normal faults), for shear stress and noting that the right-hand side of the Coulomb relation, $\{[(\sigma_1 + \sigma_2)/2] - [(\sigma_1 - \sigma_2)/2]\sin 2\phi\}\Delta\mu$, represents the driving stress, we have

$$(\sigma_1 - \sigma_3) = \frac{2\sigma_d}{\sin(2\phi)} = \frac{\gamma E}{C(1-\nu^2)\sin(2\phi)} \qquad (14)$$

Equation (14) shows the cumulative elastic differential stress consistent with an inelastic fault population strain.

[16] The driving stress typically represents an average over the depth of faulting T, as does the differential stress in (14). Using $\sigma_v = \rho g z$ and noting that $\sigma_1 = \sigma_v$ for normal faults and $\sigma_1 = \sigma_H$ for thrust faults, the value of driving stress at any given depth within the faulted domain may be calculated by using, for example, $\sigma_{dz} = (3/2\ \sigma_d/T)$ for a linear increase in σ_{dz} from zero with depth. The differential stresses given by (14) act throughout a volume without requiring that the number and sizes of faults be specified explicitly [e.g., *Jaeger and Cook*, 1979, p. 338], providing a straightforward criterion for quantitatively relating cumulative elastic stress to inelastic fault population strain.

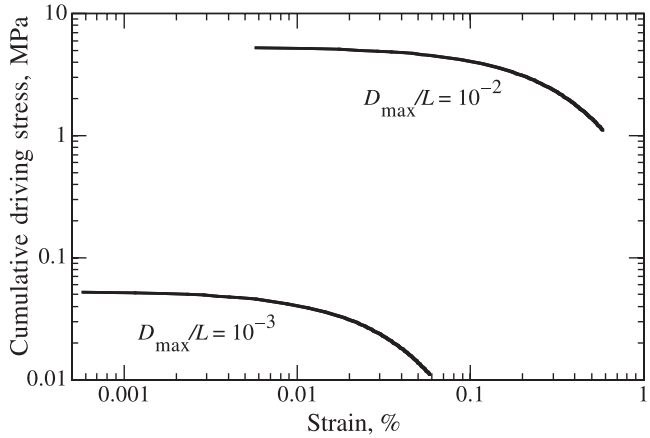

Figure 1. Cumulative elastic driving stress for fault populations at given D_{max}/L to accumulate brittle strains (equation 13). Parameters given in text; ρ_{fp} varies from 0.01 to 1.0.

5. Application to Martian Fault Populations

[17] Two examples from Mars, where measurements of fault population strains are now becoming available, illustrate the method. Spatially distributed thrust faults (including Amenthes Rupes) in the Arabia Terra region of eastern Mars define $\gamma = \sim 6 \times 10^{-3}$ [*Watters et al.*, 2000], $\rho_{fp} = 0.18$, and a fault-normal strain of 0.06% [*Schultz*, 2003]. Using the parameters given above (with $C = 0.5$ and $\delta = 30°$), $\sigma_d = 320$ MPa for constant Young's modulus (equation 10) across the faulted domain and 1.5 MPa for evolving elastic properties (equation 13). The cumulative elastic differential stresses at 1 km depth consistent with the Amenthes fault population strain are (using equation 14) $(\sigma_1 - \sigma_3) = 37$ MPa. This value for differential stress is what a Mars geodynamic model (with constant elastic properties for lithospheric rocks) should predict for the model to match the observations.

[18] Martian normal faults in the Tempe Terra region of western Mars (northern Tharsis) define $\gamma = \sim 7 \times 10^{-3}$ [*Wilkins et al.*, 2002], $\rho_{fp} = 4.3$, and a total extensional strain (from Noachian time through the present) of ~1% (S. Wilkins, pers. commun., 2002). Using the parameters above and $\delta = 50–60°$, the cumulative driving stress is $\sigma_d = 374$ MPa (equation 10) or 3 kPa (equation 13). The latter value for population driving stress is so small that the relation in (12) may be suspect for the linked faults on Tempe Terra. On the other hand, the value for cumulative elastic differential stress, $(\sigma_1 - \sigma_3) = 87$ MPa, provides a useful bound on Tharsis geodynamic models (at 1 km depth, for example,

depth of faulting of $T = 15$ km, and constant rock properties E and ν) for extension in this part of northern Tharsis.

6. Conclusions

[19] A simple means for relating planetary geodynamic models that predict elastic stress magnitudes to inelastic brittle strains obtained from observed fault populations is presented in this paper. A geodynamic model that assumes constant elastic properties for crustal rocks during the deformation (i.e., growth of fault populations) can use equation (14) with constant modulus (equation (10) to test its predictions of inelastic strain. Alternatively, models that allow rock properties to change as faulting proceeds can use (14) with (12). Examples show the magnitudes of cumulative driving stress, or cumulative elastic differential stress, that should be predicted by a model to match the observed tectonics for two areas on Mars for which the appropriate fault population data are available.

[20] **Acknowledgments.** Thanks to Juliet Crider and Daniel Mège for their careful and constructive reviews. This work was supported by a grant from NASA's Planetary Geology and Geophysics program. Scott Wilkins is thanked for discussions on extensional strain at Tempe Terra, and Tom Watters for those in Arabia.

References

Aki, K., and P. G. Richards, *Quantitative Seismology: Theory and Methods*, 932 pp., W. H. Freeman, New York, 1980.

Banerdt, W. B., M. P. Golombek, and K. L. Tanaka, Stress and tectonics on Mars, in *Mars*, edited by H. H. Kiefer, et al., pp. 249–297, Univ. of Ariz. Press, Tucson, 1992.

Bieniawski, Z. T., Classification of rock masses for engineering: The RMR system and future trends, in *Comprehensive Rock Engineering*, vol. 3, edited by J. A. Hoek and J. A. Hudson, pp. 553–573, Pergamon, New York, 1993.

Borgos, H. G., P. A. Cowie, and N. H. Dawers, Practicalities of extrapolating one-dimensional fault and fracture size-frequency distributions to higher-dimensional samples, *J. Geophys. Res.*, *105*, 28,377–28,391, 2000.

Chell, G. G., The application of post-yield fracture mechanics to penny-shaped and semi-circular cracks, *Eng. Fract. Mech.*, *9*, 55–63, 1977.

Clark, R. M., and S. J. D. Cox, A modern regression approach to determining fault displacement-length scaling relationships, *J. Struct. Geol.*, *18*, 147–152, 1996.

Cowie, P. A., and C. H. Scholz, Physical explanation for the displacement-length relationship of faults using a post-yield fracture mechanics model, *J. Struct. Geol.*, *14*, 1133–1148, 1992.

Cowie, P. A., C. H. Scholz, M. Edwards, and A. Malinverno, Fault strain and seismic coupling on mid-ocean ridges, *J. Geophys. Res.*, *98*, 17,911–17,920, 1993.

Dawers, N. H., M. H. Anders, and C. H. Scholz, Growth of normal faults: Displacement-length scaling, *Geology*, *21*, 1107–1110, 1993.

Gupta, A., and C. H. Scholz, Brittle strain transition in the Afar depression: Implications for fault growth and seafloor spreading, *Geology*, *28*, 1087–1090, 2000a.

Gupta, A., and C. H. Scholz, A model of normal fault interaction based on observations and theory, *J. Struct. Geol.*, *22*, 865–879, 2000b.

Jaeger, J. C., and N. G. W. Cook, *Fundamentals of Rock Mechanics*, 3rd ed., Chapman and Hall, New York, 1979.

Johnson, C. L., and R. J. Phillips, Constraints on the evolution of the Tharsis region of Mars (abstract) [CD-ROM], *Lunar Planet. Sci.*, *34*, 1360, 2003.

Kachanov, M., Effective elastic properties of cracked solids: Critical review of some basic concepts, *Appl. Mech. Rev.*, *45*, 304–331, 1992.

Kemeny, J., and N. G. W. Cook, Effective moduli, non-linear deformation and strength of a cracked solid, *Int. J. Rock Mech. Min. Sci. Geomech. Abstr.*, *23*, 107–118, 1986.

Kohlstedt, D. L., B. Evans, and S. J. Mackwell, Strength of the lithosphere: Constraints imposed by laboratory experiments, *J. Geophys. Res.*, *100*, 17,587–17,602, 1995.

Marone, C., Laboratory-derived friction laws and their application to seismic faulting, *Annu. Rev. Earth Planet. Sci.*, *26*, 643–696, 1998.

Mège, D., and P. Masson, Stress models for Tharsis formation, Mars, *Planet. Space Sci.*, *44*, 1471–1497, 1996.

Moore, J. M., and R. A. Schultz, Processes of faulting in jointed rocks of Canyonlands National Park, Utah, *Geol. Soc. Am. Bull.*, *111*, 808–822, 1999.

Olson, J. E., Joint pattern development: Effects of subcritical crack growth and mechanical crack interaction, *J. Geophys. Res.*, *98*, 12,251–12,265, 1993.

Phillips, R. J., et al., Ancient geodynamics and global-scale hydrology on Mars, *Science*, *291*, 2587–2591, 2001.

Pollard, D. D., and P. Segall, Theoretical displacements and stresses near fractures in rock; with applications to faults, joints, veins, dikes, and solution surfaces, in *Fracture Mechanics of Rock*, edited by B. K. Atkinson, pp. 277–349, Academic, San Diego, Calif., 1987.

Renshaw, C. E., Mechanical controls on the spatial density of opening-mode fracture networks, *Geology*, *25*, 923–926, 1997.

Scholz, C. H., Earthquake and fault populations and the calculation of brittle strain, *Geowiss.*, *15*, 124–130, 1997.

Scholz, C. H., Earthquakes and friction laws, *Nature*, *391*, 37–42, 1998.

Schultz, R. A., Understanding the process of faulting: Selected challenges and opportunities at the edge of the 21st century, *J. Struct. Geol.*, *21*, 985–993, 1999.

Schultz, R. A., Seismotectonics of the Amenthes Rupes thrust fault population, Mars, *Geophys. Res. Lett.*, *30*(6), 1303, doi:10.1029/2002GL016475, 2003.

Schultz, R. A., and H. Fossen, Displacement-length scaling in three dimensions: The importance of aspect ratio and application to deformation bands, *J. Struct. Geol.*, *24*, 1389–1411, 2002.

Segall, P., Rate-dependent extensional deformation resulting from crack growth in rock, *J. Geophys. Res.*, *89*, 4185–4195, 1984.

Segall, P., and D. D. Pollard, Joint formation in granitic rock of the Sierra Nevada, *Geol. Soc. Am. Bull.*, *94*, 563–575, 1983.

Walsh, J. B., The effect of cracks on the uniaxial elastic compression of rocks, *J. Geophys. Res.*, *70*, 399–411, 1965.

Watters, T. R., R. A. Schultz, and M. S. Robinson, Displacement-length relations of thrust faults associated with lobate scarps on Mercury and Mars: Comparison with terrestrial faults, *Geophys. Res. Lett.*, *27*, 3659–3662, 2000.

Wilkins, S. J., R. A. Schultz, R. C. Anderson, J. M. Dohm, and N. H. Dawers, Deformation rates from faulting at the Tempe Terra extensional province, Mars, *Geophys. Res. Lett.*, *29*(18), 1884, doi:10.1029/2002GL015391, 2002.

R. A. Schultz, Geomechanics-Rock Fracture Group, Department of Geological Sciences/172, Mackay School of Mines, University of Nevada, Reno, NV 89557-0138, USA. (schultz@mines.unr.edu)